applied sciences

MDPI

Article

Brain Tumor Classification Using Conditional Segmentation with Residual Network and Attention Approach by Extreme Gradient Boost

Arshad Hashmi * and Ahmed Hamza Osman

Department of Information Systems, Faculty of Computing and Information Technology in Rabigh (FCITR), King Abdulaziz University, Jeddah 21911, Saudi Arabia
* Correspondence: ahsyed@kau.edu.sa

Abstract: A brain tumor is a tumor in the brain that has grown out of control, which is a dangerous condition for the human body. For later prognosis and treatment planning, the accurate segmentation and categorization of cancers are crucial. Radiologists must use an automated approach to identify brain tumors, since it is an error-prone and time-consuming operation. This work proposes conditional deep learning for brain tumor segmentation, residual network-based classification, and overall survival prediction using structural multimodal magnetic resonance images (MRI). First, we propose conditional random field and convolution network-based segmentation, which identifies non-overlapped patches. These patches need minimal time to identify the tumor. If they overlap, the errors increase. The second part of this paper proposes residual network-based feature mapping with XG-Boost-based learning. In the second part, the main emphasis is on feature mapping in nonlinear space with residual features, since residual features reduce the chances of loss information, and nonlinear space mapping provides efficient tumor information. Features mapping learned by XG-Boost improves the structural-based learning and increases the accuracy class-wise. The experiment uses two datasets: one for two classes (cancer and non-cancer) and the other for three classes (meningioma, glioma, pituitary). The performance on both improves significantly compared to another existing approach. The main objective of this research work is to improve segmentation and its impact on classification performance parameters. It improves by conditional random field and residual network. As a result, two-class accuracy improves by 3.4% and three-class accuracy improves by 2.3%. It is enhanced with a small convolution network. So, we conclude in fewer resources, and better segmentation improves the results of brain tumor classification.

Keywords: magnetic resonance imaging; CNN segmentation; patches; CRF; XGBoost; machine learning; medical image processing; attention mechanism

Citation: Hashmi, A.; Osman, A.H. Brain Tumor Classification Using Conditional Segmentation with Residual Network and Attention Approach by Extreme Gradient Boost. *Appl. Sci.* **2022**, *12*, 10791. https://doi.org/10.3390/app122110791

Academic Editors: Jose-Maria Buades-Rubio and Antoni Jaume-i-Capó

Received: 16 September 2022
Accepted: 14 October 2022
Published: 25 October 2022

1. Introduction

The brain is the body's command center. It regulates all of the body's important operations through a massive network of connections and neurons. A brain tumor is a dangerous condition [1]. The proliferation of aberrant cells within the brain affects the nervous system and even the central spine, compromising brain function. It grows slowly, has well-defined boundaries, and spreads only rarely. It affects an estimated 700,000 persons in the United States. Secondary brain tumors are the most prevalent type of tumor [2,3]. It is both dangerous and life threatening. When cancerous cells from another organ, like the breast or lung, move into the brain, this is called a secondary brain tumor [3]. A malignant brain tumor expands to neighboring brain areas, grows swiftly, and has uneven borders. It contains cancerous cells. The World Health Organization has classified benign tumors as grade 1 and 2 low-grade tumors [4,5] and malignant tumors as grade 3 and 4 high-grade tumors [6]. In prior research, machine learning and deep learning techniques were used to classify brain tumors. In machine learning, the use of Support Vector Machine (SVM) [6,7]

and Fisher kernel function improve the accuracy in comparison to deep learning techniques such as Convolution Neural Network(CNN), Multi scale Convolution Neural Network [8], and CNN with Genetic algorithm(GA) [9].

The goal of this study is to examine how the various GBM failure patterns affect the results of second surgery. Overall survival (OS) and post-recurrence survival (PRS) were examined according to clinical factors in a prospective cohort of patients with recurrent GBM. One of the clinical features that was taken into account was the pattern of recurrence. Calculations based on the Kaplan–Meier method were used to determine survival curves; the log-rank test was applied in order to evaluate the differences in survival rates between the various curves. Patients who experienced a recurrence that was local had a longer OS than those who experienced a recurrence that was not local, with an OS of 24.1 months compared to 18.2 months, respectively (P = 0.015, HR = 1.856 (1.130–3.010)). This benefit was more pronounced in patients who had a recurrence of their cancer in their local area (P = 0.002 with HR 0.212 (95% CI: 0.081–0.552) and P = 0.029 with HR = 0.522 (95% CI: 0.289–0.942)). Patients who have recurrent GBM and are candidates for a second operation may have a different prognosis depending on the pattern of their re-occurrence [6]. Conditional deep learning is proposed here for the purpose of brain tumor segmentation, residual network-based classification, and overall survival prediction utilizing structural multimodal magnetic resonance images (MRI). First, they devised a method of segmentation based on a convolution network, and then, they used a technique called conditional random field to locate patches that did not overlap. Because of the tumor, it is imperative that these patches be applied as quickly as humanly possible. If there is overlap, the mistakes should be made larger. The residual network-based feature mapping with XG-Boost-based learning was proposed in the second half of this paper. In the second half of this paper. In the second segment, mapping characteristics [10] has been discussed.

1.1. Brain MRI Images

MRI is the most efficient and extensively used technology for diagnosing a brain tumor. MRI offers data on the human soft tissue structure, which is magnified to provide detailed views in each direction. MRI is utilized in medical imaging to show variations in soft tissues [10]. The MRI picture is used to indicate brain tumors [7].

MRI produces images with varying properties dependent on internal anatomical structures [8]. MRI is noted for its excellent picture clarity and tumor appearance precision. MRI alone cannot detect or diagnose malignancies; the segmentation of brain tumors is required for categorization [9,10]. When analyzing medical images, brain tumor segmentation is critical. MRI scanning is utilized for medical diagnostics [11]. The interpretation of MRI brain tumor images presents numerous obstacles [12]. Computational intelligence and machine learning advances allow earlier detection of brain cancers. Many methods for classifying brain cancers from MR images exist. Example: Artificial Neural Networks, knowledge-based approaches, expectation–maximization (EM), Fuzzy C Means (FCM), and SVM [7,9]. These are efficient algorithms for region segmentation and data extraction from medical pictures [12]. Brain tumors can be identified and segmented using Gaussian mixture modeling, hidden Markov random fields, and Non-Negative Matrix Factorization [13,14]. In image processing, segmentation is a challenging task due to the inefficiency of previous research and approaches, which increase overlapping and reduce feature efficiency.

Classification of Brain MRI Images

The literature proposes several techniques to classify brain tumors using MR imaging. The study [5] found that integrating 3D DWT (Discrete Wavelet Transformation) feature extraction with a Random Forest (RF) classifier improved brain tumor classification accuracy. Also used for MR image categorization are SVMs [15]. The author [13] investigated a GA-SVM hybrid system using a Gaussian RBF kernel. For this purpose, GA optimization is used. However, optimal feature extraction and selection procedures require specific

knowledge [15]. Deep learning-based methods like classification, reconstruction [16], and even segmentation [17] have lately become popular in medical picture analysis. The feature extraction method used by [18] was the VGG-16 model. A feature map was input into an LSTM recurrent neural network to classify brain cancers. The authors claim that pre-trained CNN models for feature extraction outperform GoogleNet [5], ResNet [19], and AlexNet [20]. The 2D CNN limits for brain tumor MRI categorization have recently been investigated [8]. White matter (WM), gray matter (GM), and cerebrospinal fluid (CSF) may all be recognized using a voxelwise residual network (VoxResNet) based on 3D CNN-based architecture [8]. Training results with XG-Boost are dependent on optimizing the structure and lowering complexity.

1.2. Motivation

Using Machine Learning (ML) and Deep Learning (DL) approaches, many researchers have worked on the Brain Tumor Classification (BTC) and developed numerous algorithms to analyze MRI scans in order to extract numerous potential features from the dataset [5]. Brain tumor early detection is the primary motivation of this research and analysis. The automatic segmentation and categorization of medical images are critical in diagnosing, predicting tumor progression, and therapy of brain tumors. An early detection of a brain tumor results in a more rapid response to treatment, which helps to increase patients' survival rate [19]. Manually locating and classifying brain cancers in huge medical picture collections takes a lot of effort and time. So, in the proposed approach, an efficient deep learning model is used to improve segmentation with a conditional random field, which smooths the segmentation boundary edge and improves feature mapping.

1.3. Contribution of Proposed Work

The proposed approach works on the following contribution of research. Enhancing or reducing the number of patches overlapping during the segmentation process is necessary, since the tumor is frequently of the smallest size possible. It should not overlap with other objects or patches during the process. With the conditional input via a conditional random field, the proposed research improves the edges of segmentation and creates patches based on context and semantic connection. We can further enhance the feature mapping by using residual learning or feature mapping, and then, we aggregate the results in a feature matrix. Achieving better training results with XG-Boost is dependent on optimizing the structure and lowering complexity.

The remainder of this article is structured as follows. The related work for the illustration of the brain tumor classification scheme is found in Section 2. The proposed methodology is described in detail in Section 3. Section 4 elaborates on the experimental results and discussions, and Section 5 draws conclusions.

2. Related Work

This work aims to increase the performance of brain tumor classification using MRI images. This section presents the recent works related to brain tumor classification using various machine-learning techniques, as shown in Table 1.

Research Gap

- Feature selection reduces the information, so feature selection and extraction increase false positives [10]
- Segmentation is an essential part of features, so optimize segmentation is needed for adequate classification accuracy [8]
- A normal classifier does not reduce the overlapping of features nor does it increase the false positive rate [21].

Table 1. Study of recent related work related to brain tumor classification.

Ref	Year	Aim	Methodology	Feature	Segmentation	Dataset	Limitation
[10]	2019	To improve the present system's accuracy by combining hybrid feature extraction with a regularized extreme learning machine	It contains three stages: preprocessing, feature extraction, and tumor classification. The features of brain tumors are retrieved using a hybrid technique.	The features of brain tumors are retrieved using a hybrid technique	PCA-NGIST is a hybrid feature method that employs normalized GIST descriptors with PCA to extract meaningful features from brain images without image segmentation	Brain tumor dataset (figshare.com)	PCA features merge the information, so it increases the probability of information loss
[22]	2020	To develop an effective deep multi-scale 3D CNN model to classify brain tumors into low and high grades	It has a total number of eight convolutional layers and three fast, fully connected layers. The 3D convolutional layer is used to construct a precise feature map incorporating local and global contextual information. Deep network architecture improved local optima quality.			BraTS [23]	It improves the features but ignores the segmentation
[2]	2021	An effective deep learning methodology for brain tumor classification and segmentation utilizing a multi-scale convolutional neural network	A multi-pathway CNN design was employed to segment meningioma, glioma, and pituitary tumors in MRI images. The CNN architecture classified each pixel in an MRI image (slice) using one of four possible output labels. A N * N sliding window is used to classify each pixel. Each window is processed by three convolutional pathways with three scale kernels.	Best and robust covariant features	Generative and discriminative segmentation approaches used	T1-CE MRI image dataset	The sliding window increases the overlapping pixel and causes to increase in error in detection
[21]	2021	Differential deep CNN to classify brain tumors using MR images	The differential deep CNN architecture was developed to categorize brain tumors based on magnetic resonance imaging. It has five different convolutional layers separated by five pooling layers. The differential deep convolutional network model classifies six different types of MR brain images using seven channels			(TUCMD) On request from corresponding author	In this research, no improvement in the segmentation.

3. Proposed Methodology

This section discusses the proposed approach to classify the brain tumor MRI images into meningioma, glioma, and pituitary using conditional segmentation by CNN-CRF and Resnet-XG Boost techniques. Figure 1 demonstrates the basic structure of the segmentation by CNN-CRF, whereas Figure 2 illustrates the classification and feature mapping of the Resnet-XG Boost framework.

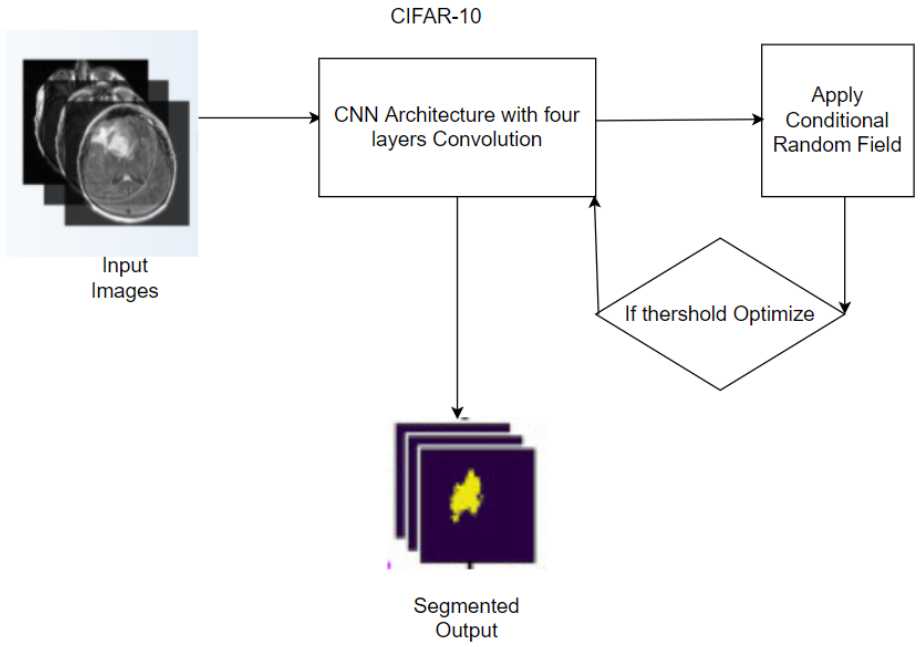

Figure 1. Segmented image by CNN-CRF.

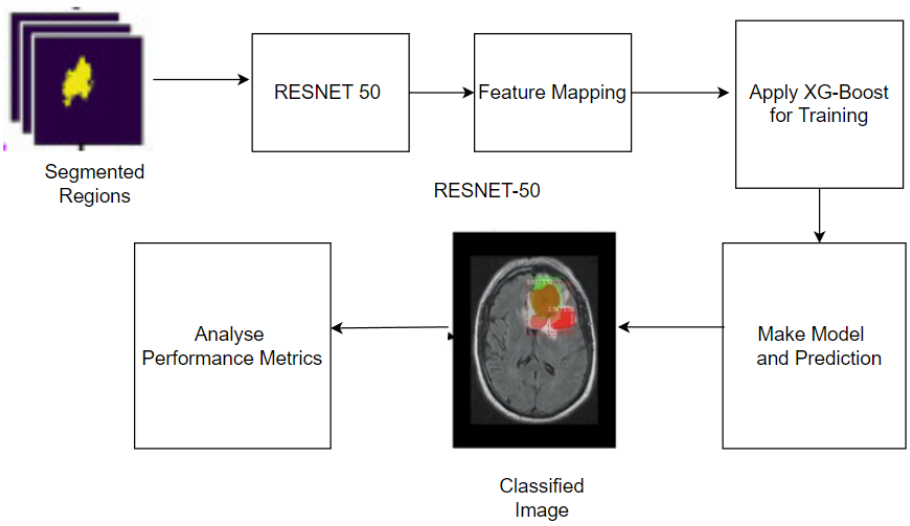

Figure 2. Classification and feature mapping framework Resnet-XG Boost.

3.1. Dataset

Clinical situations typically only allow for the acquisition and availability of a limited number of brain MRI slices, each having a significant slice gap. With such little data, creating a 3D model is challenging. As a result, the suggested method is founded on 2D slices gathered from 233 patients between 2005 and 2010 at Nanfang Hospital in Guangzhou and Tianjing Medical University, China [24]. Meningiomas (708 slices), pituitary tumors (930 slices), and gliomas (1426 pieces) are among the 3064 slices in this dataset's shared perspectives (coronal, sagittal, and axial). Additionally, this dataset has 5-fold cross-validation indices. In total, 80% (2452) of the photos are being used for training utilizing this information, while 20% (612 images) have been used to test performance. Five times the process is carried out. The pixels of the photographs are 0.49 by 0.49 mm^2 in size, with an in-plane resolution of 512 by 512. The space between the slices is 1 mm, and the slice thickness is 6 mm. The perimeter of the tumor was meticulously mapped out by three highly qualified radiologists. Each slice in the dataset is associated with an

information structure, which typically contains the patient's ID (pid), the tumor type label, which is 1 for meningioma, 2 for glioma, and 3 for pituitary tumor, the coordinates vector (x,y) of points belonging to the tumor border, and the tumor mask (Tij), which is a binary image in which the tumor positions encompass a value of 1, and the healthy ones represent by 0. The cornerstone of the training method will consist of the pair labels and features. Data augmentation via the use of an elastic transform [25] has also been used to reduce the amount of overfitting that occurs in neural networks when they are being trained. An instance of this shift is shown in Figure 3, which you may see here. The data augmentation strategy brings the total number of training pictures for each fold iteration up to 4904 from the previous 2402. In two class dataset class 1 and 2 combined and give 165 class 1 and 3 names as class2 for binary class classification.

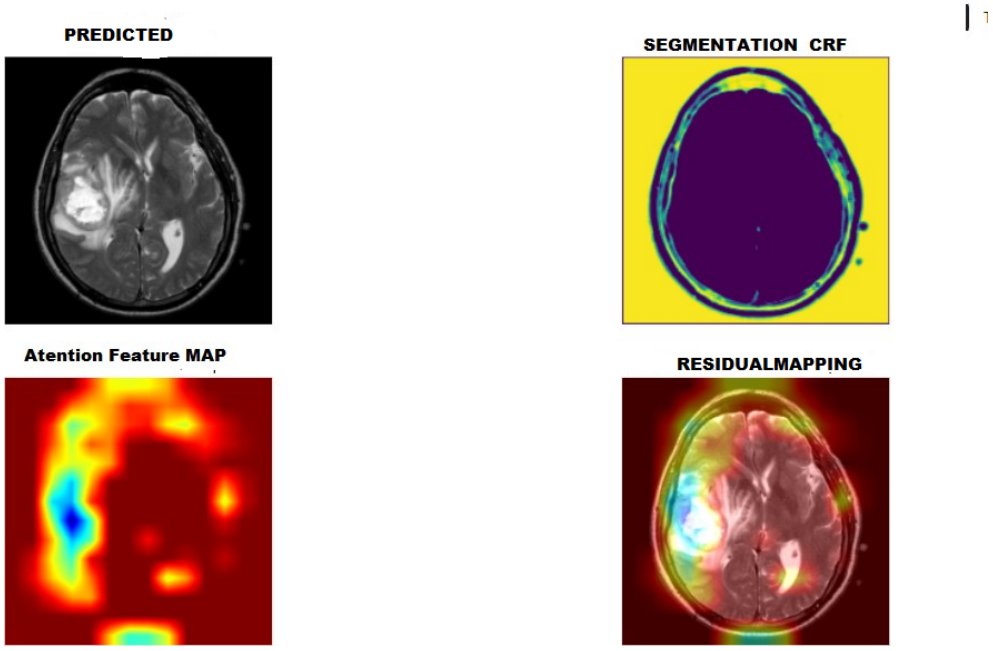

Figure 3. Three-Classes Detection Phases: Segmentation, Attention Mechanism and Activation.

3.2. Preprocessing

The preprocessing is done in two stages. The first step was to improve or reduce the noise in MRI images using Z-score. The Z-score calculates the variance between pixels and reduces it to values 0 and 1. It reduces the area of the image where the variance increases. Because the MRI image database is made up of different sizes, they must be resized to 256 by 256 normalized length. By augmenting images, we can increase the number of images in the dataset and improve the class imbalance. This was accomplished through the use of two transformation methods. The first image had a 90-degree angle. In both datasets, the second transformation was used three times more than the original to flip images vertically.

3.3. Segmentation

The Figure 1 shows the segmentation flow. CNN is used for tumor segmentation because the tumor size is so small that other approaches do not work correctly. CNN does not use the entire image for training. Instead, it was trained using patches extracted at random from images. Images are divided into patches and target categories of center points during training. The method is commonly used in biomedical image processing such as skin cancer images and mammography images [18]. The training strategy based on patches required more storage and time than the training strategy based on full-sized images. The former is preferable for tumor segmentation because small tumor areas and using full-sized images would result in false positives. CNN outperforms other methods, but it has some flaws. This paper circumvents that weakness. The limitation is that CNN segmentation is completed perfectly but with rough edges and low contrast, which sometimes misses

the tumor boundary and increases false positives. The current segmentation techniques disregard overlapping patch boundary overlaps. The overlap of patches increases the detection and localization error of tumors. The proposed CNN segmentation method maps patches, but condition-based conditional random field extracts improve the overlap. This improves the accuracy of detection by enhancing segmentation, feature mapping, and classification.

$$\in (x) = \phi(xi) + \phi(xi + xj) \quad (1)$$

$\phi(x)$ Its gradient, which computes every pixel,

$$\phi_u(x) = -logp(xi) \quad (2)$$

$p(xi)$ is labeled assignment of probabilistic parameters.

To improve segmentation, combine Conditional Random Field (CRF) with CNN. CRF is a framework for probabilistic modeling. CRF always used iterative parameter estimation techniques. We optimized the probabilistic model on his framework, using each category's contribution network properties. It is our energy function. Following the receipt, the CRF output segmentation results were modified using a variety of morphological approaches. The most connected slice was chosen as the candidate area then sections larger than 300 pixels were identified as malignant. After obtaining segmentation results for each slice, the tumor was 3D smoothed using a box filter with a 3-dimensional convolution kernel to make the segmentation findings more natural. In Segmentation, these are the following steps:

Step-1: A convolutional neural network should be used. CNN employs a four-layer CFAR-10 network.

Step-2: We used the RELU nonlinear activation function in the CNN network. This function removes unnecessary noise and provides patches as regions of interest.

Step-3: Patches are obtained by CNN, but the edges are overlapping or not clear. It is reasoned that the intensity of that region is less.

Step-4: Conditional Random Forest (CRF) improves these regions by increasing the intensity threshold and smooth edge area.

3.4. Resnet Network and Attention Mechanism

The proposed research is divided into three stages: CNN- CRF tumor segmentation, Resnet-50 tumor feature mapping, and XG-Boost ensemble learning. CDR from MRI images was classified using ResNet-50. ResNet-50 is a 50-layer residual deep learning network that was created to solve the vanishing gradient problem in CNN during backpropagation. The "vanishing gradient" problem occurs when the second-order derivatives (the gradient) matrix approaches zero in nonlinear optimization. The second issue with deepening networks is that adding layers blindly increases training error.

Deep networks can be trained using residual models. Categorical cross-entropy was the most effective way to gauge loss, as shown in Equation (2). The ResNet-50 model employs a large number of convolutions. Several filters are used to identify images (e.g., a three-pixel size filter). These filters are applied to the original image and layered on top of it. An attention layer is applied for improving the features by learning and improving the feature weights. As the focus function tests weight distribution, it estimates an array. X_i, f(X_i, X_{i+1}) features are from the second layer and f(X_i, $X_{i+1,}\cdots$, X_i + L−1) are from the L-th layer. These feature values indicate the responses of multi-scale n-grams, i.e., unigram X_i, bigram X_i X_{i+1}, and L-patches X_i $X_{i+1}\cdots X_i$ + L−1. In the focus mechanism, the filtered ensemble and reweight scale are used in unison. A scale-descriptor filter is generated to feature at each scale X_i at position i. In addition, scale reweight is used to compute the SoftMax distribution of attention weights using the descriptors as data, and it outputs weighted attribute weights for reweighing [13].

Figure 1 description is already given in Segmentation Section 3.3, but here we explained block wise significance of Figure 1. First of all by Figure 1 shows the segmentation

with convolution network using four convolution layers with 0.2 dropout and combined the features in SoftMax activation and after CNN find the segmentation edge. In this edge some edges are sharp, so for smoothing this process uses conditional random field which show in smoothing edge block. By this block refine the edges by efficient threshold which dynamically define by CRF block. Other blocks show input, middle edges, and output. In CNN input 3 by 32, there is first Conv layer 32 by 32, second Conv layer 32 by 32, third Conv layer 32 by 64 by 15, fourth Conv + pool layer 64 by 15, then flattened layer 64 by 64. Figure 2 shows the classification process segmented images, as seen in Figure 1. Then, we apply CNN variant Resnet-50, which divided it into 5 blocks: first block 7 by 7 by 64, second block 1 by 1 by 64, third block 1 by 1 by 128, fourth block 1 by 1 by 1024, and fifth block 1 by 1 by 2048. Following these features, we used the XG-Boost block to make a prediction model and then tested it on various analytical performance parameters.

Figure 3 illustrates three classes of brain tumor detection in addition to four phases and figures. The second image segmentation is on the right side, the third image has an attention mechanism on the left side, the fourth image has residual activation on the right side, and the first image prediction is on the left side, is Prediction.

3.5. Proposed Algorithm

The segmentation and classification of images are shown in the proposed Algorithms 1 and 2, respectively. Both stepwise and sequential algorithms are used in this section. Steps 1.1 through 4 of Algorithm 1 create the segmentation experiment setup and initialize the weights and parameters. Layer-wise activation function $\in (x) = \phi(xi) + \phi(xi + xj)$ is defined in step 1.5. At the *ith* iteration, CNN pixel activation $\phi(xi)$ and $\phi(xi + xj)$ add learning by the i*th* and j*th* layer. In step 1.6, remove the pixel noise x_i by applying Equation (2) $-logp(xi)$. In step 1.7, the loss function is described by referring to step 1.8. Following patch learning, proceed to step 1.9 and implement conditional random field by $E\left(X, x^{(n)}; \mu, \theta\right) - C(\ \theta; \varepsilon^i, \tau^i)$. This will define the 3D learning with $\alpha <$ Learning value (0 to 1). It reduces the edge sharpness parameters $E\left(X, x^{(n)}; \mu, \theta\right)$ by smoothing the threshold parameters $C(\ \theta; \varepsilon^i, \tau^i)$. Following this, go to step 1.10 to redefine the weights of CNN $X - E\left(y^{(n)}, x^{(n)}, \omega, \theta, \delta\right)$. Here, E represents the CRF threshold $y^{(n)}, x^{(n)}, \omega, \theta, \delta$ parameters. After updating the weight, CNN completes the segment. In Algorithm 2, transform the segmented image into a matrix pixel; then, apply Resnet-50 and $argmin\sum_{i=1}^{n} L(f_v^{(x)}, \gamma)$. This function minimizes the error of learning features and modifies the structure of $(F_0(x)) = \gamma L + \frac{1}{2}\lambda\sum_{i=1}^{L} w_i^2$ using $\frac{1}{2}\lambda\sum_{i=1}^{L} w_i^2$ by averaging weights based on training instances and setting final weights using $\frac{-\sum_{i\in L_i} g_i}{\sum_{i\in N_i} h_i + \gamma}$, where γL is the threshold. Then, we set the weight in step 2.7 $\alpha_2 \ < -(W_i, \theta)$ and test more images using these weight and analysis performance parameters.

3.6. XG-Boost(XGB)

It is a combination of both classification and regression tree sets, making it an ensemble model classification and regression tree. On the other hand, XGB [2] is used for issues of supervised learning and enhances patterns based on structure. A representation of the XG-Boost prediction model may be seen in Figure 2. The modification to XG's learning base tree structure results in an improvement to XG-Boost.

Algorithm 1: Conditional-Conv segmentation.

Input: MRI image dataset with label
Output: Segmented images

1.1 Define weight and parameters X= X_0 and $\theta = \theta_0$
1.2 Every image i, do
1.3 Run iteration = number of pixels
1.4 Apply CNN
1.5 Define activation function in Equation (1)
1.6 Calculate and cluster patch Equation (2)
1.7 Every iteration calculate cost function by step 1.8
1.8 For all patches $P_l^{[x,y,z]} < -P^{[x,y,z]_{l-1}} + \sigma[\triangle^{[x,y,z]_l} - 1]$
Where σ < Learning Parameters(0 to 1)
1.9 Optimize Conditional Random Field
$X <$ - $argmin_x\ E(X, x^{(n)};\ \mu, \theta)\ - C(\theta; \varepsilon^i, \zeta^i)$
X is finite mapping of segmentation,
$E\left(X, x^{(n)}; \mu, \theta\right)$ is pixel wise optimization,
$C(\ \theta; \varepsilon^i, \zeta^i)$ is neighbor patches
1.10 If Y $\neq Y^n$ then add
$\delta = min\ \frac{1}{2}\ \parallel X^2 \parallel$ ..... (3)
So $X_0 = X - E\left(y^{(n)}, x^{(n)}, \omega, \theta, \delta\right)$ ..... (4)
W $< -Y_0$
1.11 Update CNN weights
$\theta\ <\ -\ X +\ \delta^{(x,y,z)}$
1.12 Update Weight CNN; condu do segmentation
1.13 Return Segmented Image

Algorithm 2: Residual-Boost.

Input: Segmented images
Output: Classification of brain tumor

2.1 For every Segmented Images
2.2 $M^{(x)} < -Pixel\ Matrix$
2.3 $F_v^x\ = Resnet\ 50\ (M^{(x)})$
2.4 Initialize XG-Boost Modeling
$F_0(x) = argmin \sum_{i=1}^{n} L(f_v^{(x)}, \gamma)$..... (5)
2.5 For every instance and Leaf node N and L respectively
$\varepsilon(F_0(x)) = \gamma L + \frac{1}{2}\lambda \sum_{i=1}^{L} w_i^2$ .....(6)
2.6 For Each Leaf $W_i\ = \frac{-\sum_{i \in L_i} g_i}{\sum_{i \in N_i} h_i + \gamma}$..... (7)
2.7 Make Classifier Model $\alpha_2\ < -(W_i, \theta)$
2.8 Performance $< -\alpha_L$ (Test Set)
2.9 Analysis Performance Metrix

4. Experimental Results and Discussions

This section demonstrates the experimental results of the proposed approach. We have performed the CNN-CRF-RESNET experiments on two datasets, one in normal form and one in augmented form. On the datasets used in the experiments, ten cross-validations are employed in order to improve the model performance. The proposed method assesses results using accuracy, precision, recall, and F-Score [2]. It compared the original and augmented datasets. To carry out the procedure, Windows 10 is installed, along with an NVIDIA GeForce graphics card, a CPU running at 2.70 GHz, and 32 GB of RAM. Keras API is used in Tensor Flow to implement CNN-CRF-RESNET

4.1. Performance Metrics

The four-efficiency metrics used to evaluate the performance of the suggested method are listed in the following section. Other available performance metrics are all variants of the given performance metrics. One of the four main performance metrics is accuracy, which provides an overall picture of model performance. Other performance metrics, such as Recall, Precision and F-Score are used to analyze the true positive and true negative rate of the proposed model by using Equations (8)–(11).

Accuracy: This accuracy metric provides definitions for the labeled photos of Pituitary, Meningioma, and Glioma tumors. Equation (8) is what decides how accurate the suggested model is, and it is this equation.

$$Accuracy = \frac{TP + TN}{TP + TN + FP + FN} \tag{8}$$

In Equation (8), *TP* refers to samples that have been accurately categorized as positive, while *TN* refers to those that have been correctly classified as negative. While *FP* represents samples that have been wrongly classed as being properly classified, *FN* represents samples that have been correctly classified as being incorrectly categorized.

Recall: It is used to measure the percentage of real positive instances that we were able to accurately forecast using our algorithm. Equation (9) is used in the computation of the recall metric.

$$Recall = \frac{TP}{TP + FN} \tag{9}$$

F-Score: It is used as means of expressing harmonic mean of precision and recall. It will only accept samples that have been positively identified as pituitary, meningioma, or glioma. The F-Score is determined by applying Equation (10) to the data.

$$F\text{-}Score = \frac{2TP}{2TP + FP + FN} \tag{10}$$

Precision: It is used to measure how many of the correctly predicted cases actually turned out to be positive.

$$Precision = \frac{TP}{TP + FP} \tag{11}$$

4.2. Results and Analysis

This subsection contains the proposed system's experimental results. As mentioned previously, the suggested methodology is assessed using two distinct datasets. Additional tests, such as the F-score, recall, Precision and Accuracy, are utilized to ascertain the experimental outcomes. The proposed system consists of a CNN-CRF based network for segmentation and Resnet-XG-Boost framework for classification and feature mapping. It compared the original dataset to the augmented dataset. The experimental findings of the proposed system are also compared to those of other classification methods used in existing brain tumor detection systems. Tables 2 and 3 show the confusion matrices for the proposed BTC system's classification outcome for both datasets.

Table 2. Confusion matrix of three classes' tumors.

Meningioma	100	5	1
Glioma	3	197	0
Pituitary	6	0	300

Table 3. Confusion matrix of three classes' tumors with Augmentation.

Meningioma	2000	51	10
Glioma	58	1500	0
Pituitary	36	0	1200

4.3. Confusion Matrix

The proposed framework consists of CNN-CRF with RESNET-XG-Boost, and its results on the Three-classes datasets are shown in Table 2 using a confusion matrix. Table 3 shows the confusion matrix using an augmented dataset. The number of instances in the augmented dataset grows. In confusion matrices, non-white rows and columns represent network output classes and real classes, respectively. The correct classification is displayed along the diagonal. The larger number of non-white boxes is proportional to the number of images in the training or test set and vice versa.

In this Table 2, the experiment is analyzed using a confusion matrix. It depicts a Three-classes classification analysis. In this experiment, more than 3064 original images are used, and 10-fold cross validation is used. The dataset was divided into 80:20 by this validation process. In 90 cases, training is provided, and in ten cases, testing is conducted. Because this process is repeated ten times, the average of the entire process is used in the results. All classes perform well in the table: Meningioma detection 100, Giloma detection 197, and pituitary approximately 300 correct prediction.

Further, Table 3 depicts a Three-classes classification analysis with an augmented dataset. In this experiment, more than 4904 original images are used with 10-fold cross-validation. For the training, 90% of the dataset was used and kept 10% for the validation process. The experimental results showed all classes perform well in Table 3: Meningioma detection 2000, Glioma detection 1500, and pituitary approximately 1200 correct predictions.

4.4. Detection of Tumor

Figure 3, shown above on page 6, depicts the detection of a tumor by displaying random instances from the Three classes shown in Table 3. It shows the results of CNN-CRF-RESNET experiments on two datasets, one in normal form and one in augmented form. In Table 4 and Figure 4, different classes are used in experiments on the datasets, and ten cross-validations are employed to improve the validation. The proposed method evaluates results based on accuracy, precision, recall, and F-score. It compared the original dataset to the augmented dataset. In comparison, Three-classes' accuracy improves from the normal dataset to the augmented dataset by approximately 1.2%, precision by 1.5%, recall by 1.3%, and F-score by 1.5%. This improvement demonstrates that increasing the instances improves performance metrics in two-class datasets, including accuracy, precision, recall, and F-score. It compared the original dataset to the augmented dataset. In comparison, two-class accuracy improves by 0.3% from the normal dataset to augmented dataset, precision by 0.4%, recall by 0.23%, and F-score by 0.3%.

Table 4. Results of different datasets using the proposed approach.

Dataset	Testing Approach Cross-Validation	Accuracy	Precision	Recall	F-Score
Three Classes	10	99.56	98.56	98.12	98.45
Three Classes Augmented	10	99.45	98.78	98.12	98.56
Two Classes	10	99.12	97.34	98.12	97.89
Two Classes Augmented	10	99.89	98.12	98.45	98.1

Figure 4. Analysis of different performance metrics on Proposed approach.

Similarly, two augmented classes achieved the highest F-score value.

4.5. Comparsion with Existing

A comparison with the findings of other studies that were conducted utilizing the same T1-CE MRI image collection is the one that is most suitable to be made with our results. Table 5 shows the comparison accuracy of our techniques with that of other eight published methods. Our approach exceeds the previous suggestions by achieving an accuracy of 0.9956 for tumor categorization. In comparison, only accuracy is used because other parameters are not analyzed by the given research, and accuracy is an important parameter to analyze for the proposed model in our research.

Table 5. Comparison of Three class results.

Authors	Classification Method	Accuracy
Cheng [24]	SVM	91.2
Cheng [26]	Fisher Kernel	94.7
Abiwinanda [20]	CNN	84.1
Pashaei [19]	CNN	81
Pashaei [19]	CNN and KELM	93.6
Sultan [27]	CNN	96.1
Anaraki [28]	CNN and GA	94.2
Javier [2]	Multi-Scale CNN	97.3
Proposed	CRF-Resnet50	99.56

To validate our proposed technique and its impact on detection accuracy, we compared it to the work of other researchers who used SVM and Fisher Kernel machine learning based on detection accuracy ranging from 91% to 94%. The accuracy of CNN and CNN-based approaches ranges from 81% to 97%. Aside from that, the proposed method CRF-Resnet50 has a maximum accuracy of 99.56%. The proposed method is more effective than $O(n^2)$ when compared to existing approach complexities, but the proposed approach $O\,(NlogN)$. Existing approaches use differential CNNs for classifier tuning, which reduces accuracy to $O(n^2)$. The proposed method improved segmentation while avoiding the use of a complex network.

Segmentation is performed in existing approaches without regard to patch boundaries that overlap. The overlapping of information increases the error of tumor detection and localization. The proposed CNN segmentation approach maps in infinite nonlinear space, but conditional random field extracts condition-based finite space. This enhances detection accuracy by improving segmentation, feature mapping, and classification.

5. Conclusions

This study presents an accurate and automated brain tumor categorization method that requires little preprocessing. Deep Residual Learning is used to extract features from brain MRI images in the proposed system. The proposed method focuses on efficient segmentation by using a CNN-CRF-based approach to reduce overlapping edges. CRF provides condition-based decisions of segmented boundaries in this approach. We reduce the small tumor overlapping by other patches in non-overlapping borders. As a result, no overlapped patches improve cancer detection and detect efficient feature mapping by residual network and learning by an XG-Boost base ensemble classifier. The experiments employ two datasets: one for two classes (cancer and non-cancer) and the other for three classes (Meningioma, Glioma, Pituitary). We applied CNN-CRF-Resnet to both datasets (proposed approach), used 10-fold cross-validation, and analyzed the performance metrics. Accuracy, precision, recall, and F-Score are all important metrics, and we achieved the following values: accuracy 99.89%, precision 98.12%, recall 98.45%, and F-score 98.1% for the two classes. The following three-class experiments had improved accuracy by 99.56%, precision by 98.56%, recall by 98.12%, and F-score by 98.45%. There were improved results in the augmented approach by increasing the instances of all classes. The three classes all showed the same increase in performance. Compared to existing approaches, the two-class and three-class approaches significantly improve resources and computation. The proposed research aims to improve the overlap between patches and its effect on the mapping efficiency of features by residual network. In addition, the proposed work contributes learning and focus mechanisms for enhancing learning and features, respectively.

Author Contributions: Conceptualization, A.H.; Data Curation, A.H.; Formal Anal-ysis, A.H., A.H.O.; Acquisition, A.H.; Methodology, A.H., A.H.O.; Resources, A.H., A.H.O.; Validation, A.H., A.H.O.; Investigation, A.H.O.; Visualization, A.H., A.H.O.; Software, A.H.; Project Administration, A.H.O. Project Supervision, A.H.; Writing Original Draft, A.H.; Writing review and edit, A.H.O. All authors have read and agreed to the published version of the manuscript.

Funding: This project was funded by the Deanship of Scientific Research (DSR) at King Abdulaziz University, Jeddah, under grant no (G: 383-830-1442).

Institutional Review Board Statement: Not applicable.

Informed Consent Statement: Not applicable.

Data Availability Statement: Not applicable.

Acknowledgments: This project was funded by the Deanship of Scientific Research (DSR) at King Abdulaziz University, Jeddah, under grant no (G: 383-830-1442) . The authors, therefore, acknowledge with thanks DSR for technical and financial support.

Conflicts of Interest: The authors declare no conflict of interest. The funders had no role in the design of the study; in the collection, analysis, or interpretation of data; in the writing of the manuscript, or in the decision to publish the results

References

1. Pasqualetti, F.; Montemurro, N.; Desideri, I.; Loi, M.; Giannini, N.; Gadducci, G.; Malfatti, G.; Cantarella, M.; Gonnelli, A.; Montrone, S.; et al. Impact of recurrence pattern in patients undergoing a second surgery for recurrent glioblastoma. *Acta Neurol. Belg.* **2022**, *122*, 441–446. [CrossRef] [PubMed]
2. Díaz-Pernas, F.J.; Martínez-Zarzuela, M.; Antón-Rodríguez, M.; González-Ortega, D. A deep learning approach for brain tumor classification and segmentation using a multiscale convolutional neural network. *Healthcare* **2021**, *9*, 153. [CrossRef] [PubMed]
3. Montemurro, N.; Fanelli, G.N.; Scatena, C.; Ortenzi, V.; Pasqualetti, F.; Mazzanti, C.M.; Morganti, R.; Paiar, F.; Naccarato, A.G.; Perrini, P. Surgical outcome and molecular pattern characterization of recurrent glioblastoma multiforme: A single-center retrospective series. *Clin. Neurol. Neurosurg.* **2021**, *207*, 106735–106735. [CrossRef] [PubMed]
4. Usha, R.; K. SVM classification of brain images from MRI scans using morphological transformation and GLCM texture features. *Int. J. Comput. Syst. Eng.* **2019**, *5*, 18–23. [CrossRef]

5. Khan, M.A.; Ashraf, I.; Alhaisoni, M.; Damaševičius, R.; Scherer, R.; Rehman, A.; Bukhari, S.A.C. Multimodal brain tumor classification using deep learning and robust feature selection: A machine learning application for radiologists. *Diagnostics* **2020**, *10*, 565–565. [CrossRef] [PubMed]
6. Mathew, A.R.; Anto, P.B. Tumor detection and classification of MRI brain image using wavelet transform and SVM. In Proceedings of the 2017 International Conference on Signal Processing and Communication (ICSPC), Coimbatore, India, 27–28 July 2017; pp. 75–78.
7. Hamiane, M.; Saeed, F. SVM classification of MRI brain images for computer-assisted diagnosis. *Int. J. Electr. Comput. Eng.* **2017**, *7*, 2555–2555. [CrossRef]
8. Mohan, G.; Subashini, M.M. MRI based medical image analysis: Survey on brain tumor grade classification. *Biomed. Signal Process. Control* **2018**, *39*, 139–161. [CrossRef]
9. Wadhwa, A.; Bhardwaj, A.; Verma, V.S. A reviewon brain tumor segmentation of MRI images. *Magn. Reso Nance Imaging* **2019**, *61*, 247–259. [CrossRef] [PubMed]
10. Gumaei, A.; Hassan, M.M.; Hassan, R.; Alelaiwi, A.; Fortino, G. A Hybrid Feature Extraction Method with Regularized Extreme Learning Machine for Brain Tumor Classification. *IEEE Access* **2019**, *7*, 36–266. [CrossRef]
11. Amin, J.; Sharif, M.; Yasmin, M.; Fernandes, S.L. A distinctive approach in brain tumor detection and classification using MRI. *Pattern Recognit. Lett.* **2020**, *139*, 118–127. [CrossRef]
12. Sharif, M.; Tanvir, U.; Munir, E.U.; Khan, M.A.M. Brain tumor segmentation and classification by improved binomial thresholding and multi-features selection. *J. Ambient. Intell. Humaniz. Comput.* **2018**, 1–20. [CrossRef]
13. Swati, Z.N.K.; Zhao, Q.; Kabir, M.; Ali, F.; Ali, Z.; Ahmed, S.; Lu, J. Brain tumor classification for MR images using transfer learning and finetuning. *Comput. Med. Imaging Graph.* **2019**, *75*, 34–46. [CrossRef] [PubMed]
14. Saha, C.; Hossain, M.F. MRI brain tumor images classification using K-means clustering, NSCT and SVM. In Proceedings of the 2017 4th IEEE Uttar Pradesh Section International Conference on Electrical, Computer and Electronics (UPCON), Mathura, India, 26–28 October 2017; pp. 329–333.
15. Mukambika, P.S.; Rani, K.U. Segmentation and classification of MRI brain tumor. *Int. Res. J. Eng. Technol. IRJET* **2017**, *4*, 683–688.
16. Bhanumathi, V.; Sangeetha, R. CNN Based Training and Classification of MRI Brain Images. In Proceedings of the 2019 5th International Conference on Advanced Computing & Communication Systems (ICACCS), Coimbatore, India, 15–16 March 2019; pp. 129–133.
17. Boustani, A.E.; Aatila, M.; Bachari, E.E.; Oirrak, A. MRI brain images classification using convolutional neural networks. In *International Conference on Advanced Intelligent Systems for Sustainable Development*; Springer: Cham, Switzerland, 2019; pp. 308–320.
18. Paul, J.S.; Plassard, A.J.; Landman, B.A.; Fabbri, D. Deep learning for brain tumor classification. In *Medical Imaging 2017: Biomedical Applications in Molecular, Structural, and Functional Imaging*; SPIE: Bellingham, WA, USA, 2017; Volume 10137.
19. Pashaei, A.; Sajedi, H.; Jazayeri, N. BrainTumor Classification via Convolutional Neural Network and Extreme Learning Machines. In Proceedings of the 8th International Conference on Computer and Knowledge Engineering (ICCKE), Mashhad, Iran, 25–26 October 2018; pp. 314–319.
20. Abiwinanda, N.; Hanif, M.; Hesaputra, S.T.; Handayani, A.; Mengko, T.R. Brain tumor classifification using convolutional neural network. In *World Congress on Medical Physics and Biomedical Engineering*; Springer: Singapore, 2018, pp. 183–189.
21. Kader, I.A.E.; Xu, G.; Shuai, Z.; Saminu, S.; Javaid, I.; Salim Ahmad, I. Salim Ahmad I. Differential Deep Convolutional Neural Network Model for Brain Tumor Classification. *Brain Sci.* **2021**, *11*, 8001442. [CrossRef] [PubMed]
22. Mzoughi, H.; Njeh, I.; Wali, A.; Slima, M.B.; Benhamida, A.; Mhiri, C.; Mahfoudhe, K.B. Deep Multi-Scale 3D Convolutional Neural Network (CNN) for MRI Gliomas Brain Tumor Classification. *J. Digit. Imaging* **2020**, *33*, 7522155. [CrossRef] [PubMed]
23. Menze, B.H.; Jakab, A.; Bauer, S.; Kalpathy-Cramer, J.; Farahani, K.; Kirby, J.; Burren, Y.; Porz, N.; Slotboom, J.; Wiest, R. The multimodal brain tumor image segmentation benchmark (brats). *IEEE Trans. Med. Imaging* **2014**, *34*, 1993–2024. [CrossRef] [PubMed]
24. Cheng, J.; Huang, W.; Cao, S.; Yang, R.; Yang, W.; Yun, Z.; Wang, Z.; Feng, Q. Enhanced performance of brain tumor classifification via tumor region augmentation and partition. *PLoS ONE* **2015**, *10*, e0140381.
25. Ge, C.; Gu, I.Y.; Jakola, A.S.; Yang, J. Deep Learning and Multi-Sensor Fusion for Glioma Classification Using Multistream 2D Convolutional Networks. In Proceedings of the 40th Annual International Conference of the IEEE Engineering in Medicine and Biology Society (EMBC), Honolulu, HI, USA, 18–21 July 2018; pp. 5894–5897.
26. Cheng, J.; Yang, W.; Huang, M.; Huang, W.; Jiang, J.; Zhou, Y.; Yang, R.; Zhao, J.; Feng, Q.; Chen, W. Retrieval of brain tumors by adaptive spatial pooling and fifisher vector representation. *PLoS ONE* **2016**, *11*, e0157112.
27. Sultan, H.H.; Salem, N.M.; Al-Atabany, W. Multi-classifification of brain tumor images using deep neural network. *IEEE Access* **2019**, *7*, 69215–69225. [CrossRef]
28. Anaraki, A.K.; Ayati, M.; Kazemi, F. Magnetic resonance imaging-based brain tumor grades classifification and grading via convolutional neural networks and genetic algorithms. *Biocybern. Biomed. Eng.* **2019**, *39*, 63–74. [CrossRef]